Thesis

The Influence of H2AX and γH2AX on Chromatin Condensation

Submitted by

Sarah Samaya Norskog

Department of Biochemistry and Molecular Biology

In partial fulfillment of the requirements

For the Degree of Master of Science

Colorado State University

Fort Collins, Colorado

Summer 2010

COLORADO STATE UNIVERSITY

May 28th, 2010

WE HEREBY RECOMMEND THAT THE DISSERTATION PREPARED UNDER OUR SUPERVISION BY SARAH SAMAYA NORSKOG ENTITLED "THE INFLUENCE OF H2AX AND γH2AX ON CHROMATIN CONDENSATION" BE ACCEPTED AS FULFILLING IN PART REQUIREMENTS FOR THE DEGREE OF MASTERS OF SCIENCE.

Committee on Graduate Work

Karolin Luger

Mark Zabel

Advisor: Jeffrey Hansen

Department Chairman: Shing Ho

ABSTRACT OF THESIS

THE INFLUENCE OF H2AX AND γH2AX ON CHROMATIN CONDENSATION

Chromatin composition and structure are essential for the condensation of the genome and the regulation of a wide range of cellular activities. Chromatin condensation is thought to be controlled predominantly through interactions mediated by the unstructured amino terminal domains of the core histones H4, H3, H2A and H2B. In addition to the amino terminal domain, histone H2A contains an unstructured carboxyl terminal domain. Multiple H2A variants, many differing from major type H2A in this C-terminal domain sequence, have been identified. The most studied of variant is H2AX, which contains a conserved serine residue that becomes phosphorylated following double strand DNA breakage (γH2AX). Although the phosphorylation of the H2AX has been identified as a key step in major genomic activities, the basic mechanism by which it functions remains controversial. Here, I have determined the structural role of H2AX and γH2AX using *in vitro* assays which utilize defined nucleosomal arrays. H2AX and γH2AX alter chromatin folding under high salt concentrations but show no discernable differences in low concentrations of salt or under conditions which favor oligomerization. The phosphorylation of H2AX does not alter the folding or oligomerization relative to the

unphosphorylated form, indicating γH2AX more likely functions as a signaling and recruitment motif rather than as a chromatin secondary structure remodeling factor.

Sarah Samaya Norskog
Department of Biochemistry and Molecular Biology
Colorado State University
Fort Collins, CO 80523
Summer 2010

Acknowledgements

The past five years I have spent in the Hansen Lab have been invaluable to me and for this my deepest appreciation goes out to all of its members. I would first and foremost like to thank Dr. Steve McBryant, my phenomenal mentor for of his support and wisdom over the past years. Not only has his mentoring taught me technique and theory, but it is working with him that has taught me to think like a scientist. I would also like to thank Dr. Heather Szerlong and Troy Sorensen for their always appreciated guidance and suggestion along the way. I would like to thank Dr. Jeff Hansen for all of the opportunities he has given me. Finally, thank you to my family for their constant support and endless encouragement.

Table of Contents

Introduction and Significance

Oscar Ferandez-Capetillo called H2AX the histone guardian of the genome because of its prevailing ability to meditate DNA repair in distinct DNA metabolic pathways. It is because of this important role that the phosphorylation of the serine located four residues from the carboxyl terminus of this H2A histone variant has been the focus of much research (for review see Fernandez-Capetillo, 2004). These studies continue to provide new details of the signaling repair processes that take place shortly after a DNA double strand break occurs. Recent studies focused on phosphorylated H2AX, referred to as γH2AX, have led to the creation of new diagnostic tools, used in identifying harmful cellular damage and cancer treatment efficacy. γH2AX has been identified as having a central role in many chromatin activities including DNA repair, non-homologous end joining (NHEJ), variable diversity joining (VDJ) of antibody heavy and light chains in the cells of the immune system and meiotic recombination [2-5]. The kinases that phosphorylate the carboxyl-terminal domain of H2AX and the protein complexes that are recruited to this modification have been well characterized [6-9]. Although there is a great deal of data focusing on this modification, the exact mechanism by which γH2AX functions in hastening/facilitating DNA repair is still not fully understood.

At present time papers have been published supporting the notion that γH2AX functions solely as a binding site and recruitment signal for DNA repair complexes [7,10,11]. However, other papers have demonstrated and/or suggested that γH2AX causes a

conformational change in the chromatin, thus allowing loosening of the chromatin to facilitate DNA repair [3]. It has been shown that the phosphorylation of H2AX is required for the recruitment of many known repair proteins or repair signaling proteins to the site of DNA damage [7,12]. However, it is unknown whether it is the addition of the phosphoryl group that creates a binding site or if the phosphoryl group changes the local conformation of the chromatin architecture which allows for binding access to the DNA.

To fully understand the reactions involved in DNA repair, it is important to determine the role that H2AX and γH2AX plays in this process. The following research is focused on elucidating the effect, if any, that H2AX and its phosphorylated form have on chromatin condensation, in the hope of creating a fuller understanding of its role in DNA repair. A better understanding of γH2AX will facilitate a more complete view of many genomic metabolic processes, and will allow researchers to better utilize this modification in oncological studies and possibly in the development of novel cancer diagnostics.

Chromatin and the Nucleosome

In eukaryotic cells genetic information is organized into chromatin through the wrapping of DNA around a disk-shaped protein assembly to form nucleosomes [13]. These nucleosomes and intervening "linker" DNA are able to fold into higher order structures to control access to the underlying genomic DNA [14-16]. The nucleosome structure allows DNA molecules, which are very long (about 2 meters of total DNA length in each human cell) and negatively charged to condense into the ~10μm nucleus and also to maintain the dynamic ability to locally and globally decondense. The display or shielding of DNA through chromatin loosening or condensation, respectively, is important for major

cellular functions like gene transcription, gene/chromosome replication, DNA repair and gene silencing. This higher order chromatin structure allows nucleosomes to control what genes or regions of chromosomes are available to be recognized, bound, transcribed and replicated, and which genes are condensed and metabolically silenced.

The nucleosome core particle, the fundamental building block of chromatin, consists of 146 base pairs of DNA wrapped around a core histone octamer [17] made up of two H2A-H2B dimers and one H3-H4 tetramer (Fig. 1). The DNA is wrapped around this spool-like protein octamer in a left-handed manner, completing approximately 1.65 superhelical turns [17,18]. The DNA between nucleosomes, called linker DNA, ranges from 20 to 80 base pairs in length allows for linker histone binding [19,20] and higher order chromatin structure formation (see below).

All core histones contain a folded domain and an unstructured amino-terminal domain, NTD; which range from ~14-40 amino acids in length. H2A is the only core

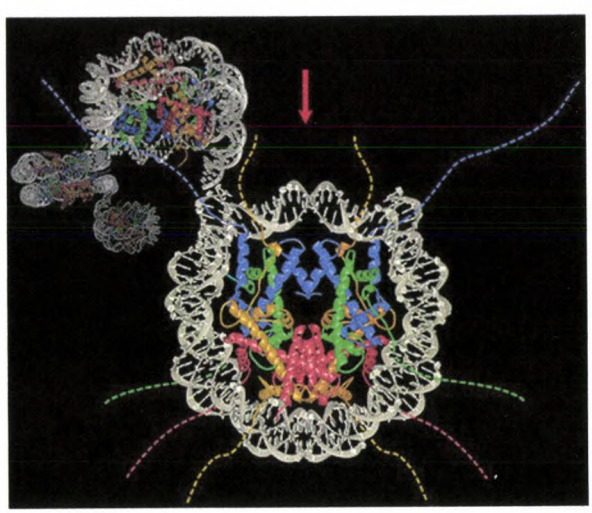

Figure 1. Ribbon diagram of the nucleosome core particle obtained from the X-ray structure. DNA (gray) is shown wrapping around the histone octamer, made up of H2A (yellow), H2B (red), H3 (blue) and H4 (green). Unstructured tail domains are represented by colored dashed lines. The red arrow indicates dyad axis as well as location of H2A CTDs. Figure modified from Luger Lab website http://lugerlab.bmb.colostate.edu/Publications.html

histone to also have a significant carboxyl terminal domain, CTD, which is typically 8-13 amino acids in long in mammals The folded domains all share a common structure of three alpha helices connected by two loops, called the histone fold motif. Interactions between the histones allow for the formation of the H2A-H2B dimer and H3-H4 tetramer structures, organized in histone 'hand-shake motifs', due to their head-to-tail orientation [21]. Two dimers of H2A-H2B bind the H3-H4 tetramer completing the flattened disk structure [18]. The unstructured amino and carboxyl terminal domains extend outward from the nucleosome core, either from between the gyres of the DNA or outside the DNA [22], and are capable of interacting with nucleosomal or linker DNA [23,24], and other proteins, including other histones [25,26]. It is the interactions of these histone terminal domains that drive the formation of higher order structure of chromatin [27,28]. While the role of the histone amino terminal domains (NTDs) in chromatin dynamics has been extensively studied for more than two decades [13,14,28-31], the influence of the H2A carboxyl terminal domain (CTD) on the structure of chromatin has not been definitively determined.

Chromatin Fiber Dynamics

Intact nuclei and chromatin extracted from the nuclei of living cells have been known for nearly 50 years to undergo major structural rearrangements when the solution conditions are altered [32-35]. Salt-dependent condensation of chromatin occurs via two primary pathways, folding and self-association [14,28]. Folding occurs via short-range, intra-fiber nucleosome-nucleosome interactions along a linear strand of chromatin. Folding of chromatin results in the formation of moderately folded material and extensively folded material, seen as the canonical 30nm fiber [28,36,37] (Fig. 2). Self association occurs via

long range, inter-fiber interactions (Fig. 2) [13,14,38]. Because the range of salt needed to both fold and self-associate chromatin is so limited (i.e. folding at ~0.25-1.5mM and self-association at ~2.5 mM MgCl2) the compaction of the chromatin can be readily oscillated between the highly condensed and the more 'open' conformation by subtle changes in the ion concentration within the nucleus. These structural changes are mediated largely in part by protein-protein and protein-DNA interactions through the histone NTDs [18,31,39-42]. Some of the most convincing evidence of this was produced by Richmond and coworkers through novel deletions of the NTDs. When the NTD of histone H4 was removed full folding was not observed [39]. The importance of the NTDs for chromatin condensation has been further corroborated by different labs, using multiple techniques. For example, an *in vitro* cross-linking assay developed by the Hayes lab determined that the H3 NTD is involved in the long range interactions of self association [42]. Adding to this, another

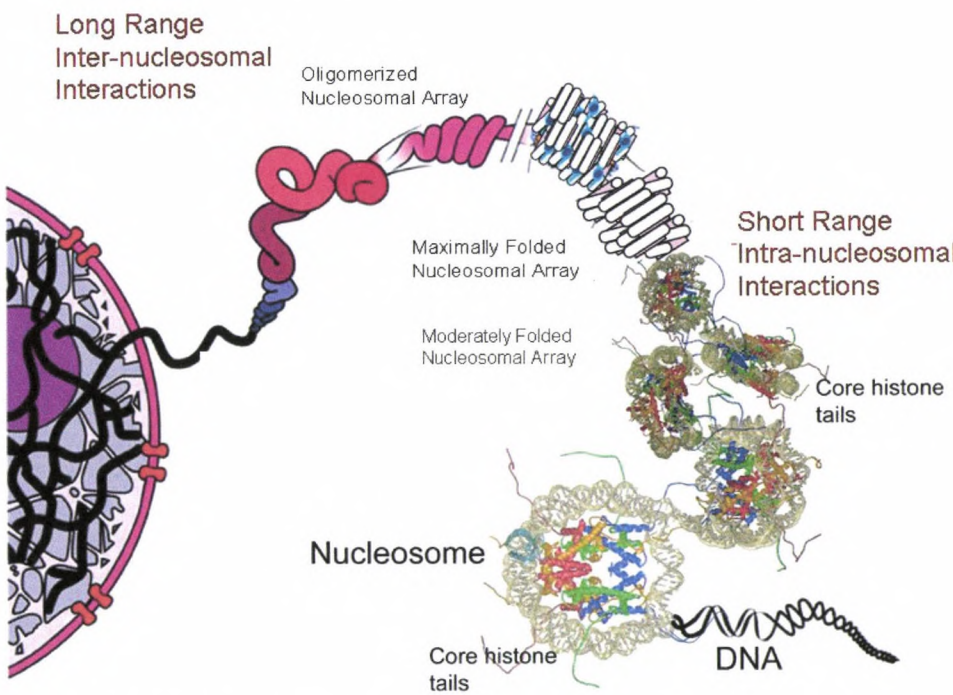

Figure 2. Chromatin condensation with in the nucleus. Nucleosomal array model is signified at moderately folded, maximally folded and oligomerized compaction. Figure modified from Chakravarthy, 2005.

cross-linking study from the Hayes lab showed that the H4 NTD interacted with both DNA and the histone fold of H2A, and that these interactions were dependent on the nature of the condensed array [43]. Thus, the tails are dynamically engaged with DNA and protein components of the nucleosome during all phases of chromatin condensation.

In addition, a host of non-histone proteins (chromatin architectural proteins) also interact with the native chromatin, acting along with the core histones to govern the dynamic accessibility of the chromatin fiber [44-47]. *In vivo,* the two conformations, 'highly condensed' and 'open', are referred to as heterochromatin and euchromatin, respectively. Both folding and self association can be measured using *in vitro* assays and highly pure and well-defined nucleosomal arrays to mimic native chromatin fibers. Such *in vitro* studies have been shown to closely correlate with studies using native chromatin (extracted from the nuclei of living cells) in that the salt-dependent transitions are nearly identical in nature [48]. Nucleosomal arrays consist of linear DNA molecules made up of tandem repeats of high-affinity nucleosomal binding sequences [49,50] bound by purified (native or recombinant) histone octamers.

Folding assays are carried out in low concentrations of salt (0.25-1.5mM MgCl2) and result in an overall shortening of the array, as the DNA that enters and leaves the nucleosomes come in closer contact, forming an irregular zig-zag structure [51]. The degree of folding is calculated using sedimentation velocity data from the analytical ultracentrifugation and the characterization of chromatin structure [52,53]. In this assay, nucleosomal arrays are sedimented in a high centrifugal field, and their movement is detected in real time using UV absorbance (260nm to detect the DNA chromophores). When salt is added to a nucleosome array, the array becomes shorter and thicker (with no

appreciable change in mass), thus the frictional resistance to movement has decreased and the array will sediment more quickly, resulting in a sample with a higher sedimentation coefficient. Folding occurs to two distinct capacities. Intermediately folded material forms in lower concentrations of salt, while maximal folding follows as salt concentrations increase. The hallmark sedimentation coefficients for these two conformations are 40S and 55S respectively [28,54,55].

Self-association assays measure the degree to which nucleosomal arrays form large insoluble aggregates in slightly higher salt concentrations (2.5-10mM MgCl2). This transition is readily reversible by dialyzing the sample to remove the salt [56] and is the direct result of inter-nucleosomal interactions mediated by the histone NTDs (in particular the H4 NTD appears to be of utmost importance for this transition) [14,57,58]. Self-association is measured using differential centrifugation in a microfuge and UV spectrophotometry to calculate the percent of sample that self-associates and is pelleted out of solution at relatively low centrifugal forces [28].

Post Translational Modification of Histone Terminal Domains

Histone terminal domains are commonly modified post-translationally and these modifications serve a multitude of functions. Over 60 different residues of the four core histone terminal domains have been identified to have post translational modifications [59]. Common modifications include acetylation [60], methylation [61], phosphorylation [61], ubiquitilation [62], sumoylation [63], and poly ADP-ribosylation [64]. These enzymatic modifications occur as a result of a variety of upstream signal transduction pathways, and tend to be reversible, further adding to the dynamic nature of the chromatin fiber.

One of many ways to simplify the effects of these histone modifications was proposed by Dr Tony Kouzarides at the University of Cambridge, UK [59]. In this analysis Dr. Kouzarides sets up two major effects of histone tail post translational modifications. The first is the "establishment of global chromatin environments," which refers to the formation and partitioning of heterochromatin and euchromatin. Thus, these modifications act to globally condense or de-condense chromatin. The second category is referred to as "the orchestration of DNA-based biological tasks." These modifications control the structure and unraveling of chromatin in local or regional sections of the chromosome, allowing specific DNA metabolic functions such as DNA repair or replication to occur. This control of biological tasks often requires additional cellular machinery to function within this defined chromatin architecture.

The mechanism of action of these post translational modifications (PTM) varies between modifications and, particularly when taken in combination, can be complex. Certain modifications are able to recruit proteins or protein complexes by using the now-altered amino acid chemistry to create novel binding sites on the chromatin [59]. Histone PTMs may also affect the interactions between the core histones, DNA (nucleosomal as well as linker DNA), adjacent nucleosomes and/or a combination of these. For example, the acetylation of lysine 16 on histone H4 inhibits the binding of the ACF protein complex and reduces the ability of chromatin to form folded and self associated structures [65]. Modifications that alter the charge of the histone terminal domains tend to have the greatest effects of chromatin structure and interactions, as they likely alter the interactions between the negatively charged DNA and neighboring histones which are largely electrostatic in nature. Studies using *in vivo* and *in vitro* systems have shown

these charge-based modifications are capable of decreasing the ability of chromatin to form higher order structures [59,66].

Histone H2A and its Variant H2AX

The major-type core histone H2A is the only such core histone with a significant CTD (13 amino acids in length). The CTD protrudes from the nucleosome at the dyad axis, where the DNA enters and exits the nucleosome (Fig. 1). The CTD may contact portions of DNA wrapped around the nucleosome, as well as some linker DNA between the nucleosomes and even the linker histone, H1. These contacts with linker DNA are attenuated in the presence of linker histone, H1 [67].

More variants of the H2A histone have been identified than any other histone [68]. These variants have high variability in their CTDs and/or NTDs, likely resulting in diversity of functions. The disordered tail domains of the H2A variants, like H2AX [69-72], H2AZ [70-72] and MacroH2A [71,72], may regulate chromatin pathways via two interconnected mechanisms. First, the primary sequence of these unstructured regions allows for novel binding sites for DNA and/or other proteins and complexes, likely simultaneously. Secondly many PTM sites have been identified on the tail regions, with the potential for further enhancing the dynamic regulation that the H2A variants may have in both structure and function. For example, macroH2A has a greatly extended CTD compared to the major type H2A [71]. This domain contains a region that directly binds PARP-1 [73]. The macro H2A CTD also contains multiple PTM sites, such as S137 which when phosphorylated alters the structure of the CTD, inhibiting RNA binding [71]. It is likely that both factor binding and PTMs work together to establish the dynamic functions of the H2A variants.

Despite the fact that only a handful of the 20 amino acids are represented in the N- and C-terminal regions of the core histones, the highest degree of sequence divergence is seen there. These regions have long been recognized as lacking regular secondary structure in solution, though have been shown to adopt regular folded structures when bound to DNA or in the presence of structure-inducing solvents such as triflouroethanol or sodium perchlorate (for review see Hansen, 1998) [74]. Proteins or regions of proteins which lack regular secondary structure under native conditions are often referred to as 'intrinsically disordered', or 'natively disordered'. Regions of intrinsic disorder are thought to play a large role in cell signaling and function in most necessary biological processes [75,76]. We commonly think about protein secondary and tertiary structure as the guiding factors in function, but innumerable proteins or protein domains lacking well-defined secondary structure are known to carry out key regulatory functions. Indeed, intrinsic disorder has distinct advantages compared to folded confirmations. The ability of an unfolded protein to adopt more than one binding conformation allows it to bind multiple targets. The binding affinity can be further controlled through the thermodynamics of ligand binding and induced folding due to ligand binding or even PTM [77]. With this, it is easy to envision that the unstructured CTD and NTDs of the H2A variants increase the ability of these proteins to regulate chromatin architectural pathways.

Of the H2A variants, H2AX has been the most studied [2,5,7,78]. On average, 10% of the total H2A in a cell consists of the H2AX variant, however this percent can range from 2.5 to 25% depending on species, cell type and amount of DNA damage within the cell [69]. The distribution of H2AX within chromatin remains unclear. It has not been

identified if H2AX localizes to specific regions of the chromatin or if its presence is distributed evenly through out the chromatin. It is also unknown if H2AX prefers to form homotypic nucleosomes consisting of two copies of H2AX or heterotypic octamers consisting of one copy of major type H2A and one copy of H2AX [69]. Speculation of random distribution throughout the genome is the current, common assumption, allowing for a rapid, local response to DNA damage throughout the genome.

H2AX varies from wildtype H2A most distinctly in its CTD; the H2AX CTD has a different primary sequence and is longer. The extended CTD of H2AX contains a highly conserved serine-glutamine-glutamic acid sequence, referred to as the SQE region. This conserved region positions a serine residue four amino acids from the carboxyl-terminus. Lower eukaryotes such as *Saccharomyces cerevisiae* do not have the H2AX variant; instead the major type H2A of these species contains the SQE section.

The length of the H2AX CTD varies between species and is thought correlate with the complexity of evolution, meaning more evolved species like humans and mice

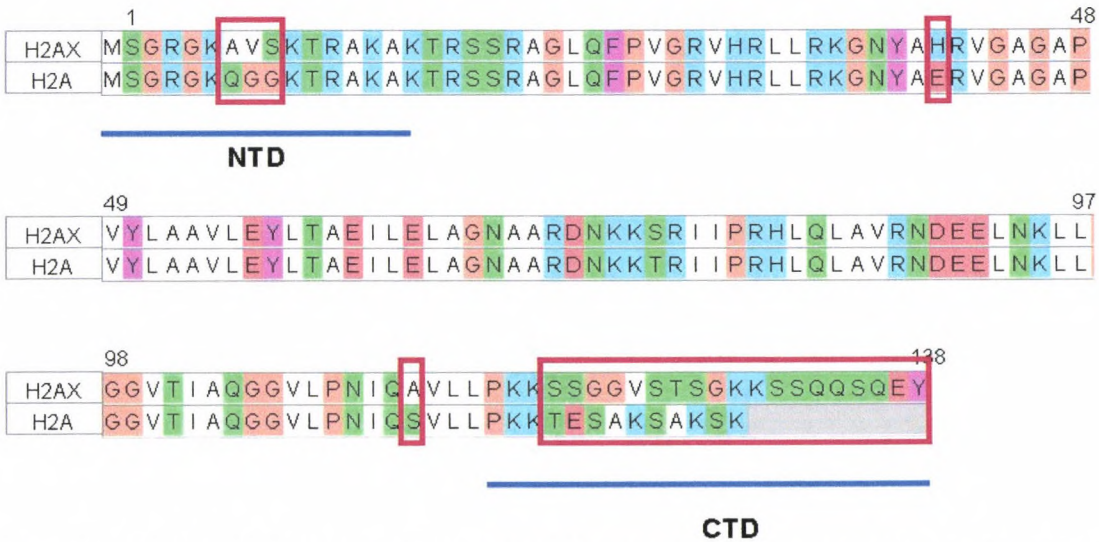

Figure 3 Amino Acid Sequence Alignment of *Xenopus laevis* H2A and H2AX. Sequence variations indicated by red boxes. Residues color coded as: polar positive is blue, polar negative is red, polar neutral is green, non-polar aliphatic is grey, non polar aromatic is purple or brown. Alignment produced using cinema 2.1

have longer CTDs (26 amino acids in length) compared to less evolves species like *Giardia intestinalis* (10 amino acids in length) [69]. This link to evolutionary complexity may be related to linker DNA length between nucleosomes which has been shown to increase with species development [79]. Since the residues found in the extended region of the CTD are rich in prolines, glycines and other hydrophilic amino acids, the tail is likely unstructured and flexible. Longer linker DNA allows for a longer H2AX CTD to fit with in the chromatin without causing steric hindrance [69], or may allow for more contact to occur between the CTD and linker DNA .

Other key differences between major-type H2A and H2AX are three amino acids substitutions in the NTD (Q6A, G7V, G8S) and the two within the globular domain (E41H and S113A) (Fig. 3). The most notable change, with the possibility of distinguishing H2A from H2AX, is the E41H substitution. The glutamic acid at residue 41 in H2A is known to hydrogen bond with asparagine 39 (N38) on the other H2A in the octamer complex [18]. A substitution from glutamic acid to histidine (E41H) would not only change the charge from negative to positive within the binding pocket, but would also negate the hydrogen bond to the other H2A (Fig 4). Absence of this interaction may increase nucleosome flexing, which in turn could impact the ability of the chromatin to form more highly condensed structures [69].

In many organisms A38 varies between H2A and H2AX by an asparagine to histidine substitution. This residue is involved in the same H2A-H2A interaction as well as hydrogen bonding with H79 on the other H2B. The addition of a charged residue that can not form the same hydrogen bonds may: 1) weaken intra-octamer binding, 2) facilitate the removal of one or both of the H2A-H2B dimers, and/or 3) alter chromatin

condensation [69,80]. However, in *Xenopus laevis* (the species-type of the histones used for this research) the 38th residue is asparagine for both major type H2A and H2AX, so any interference in the H2A-H2A/H2B interaction likely would be due to E41H.

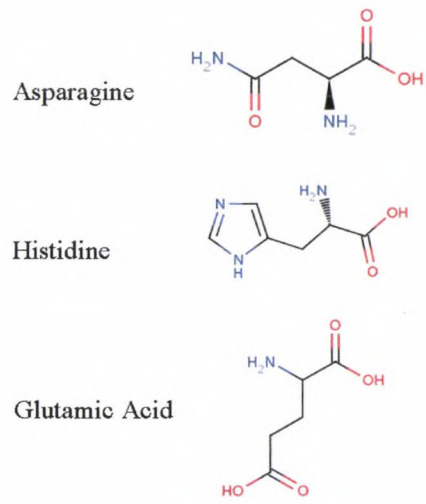

Figure 4 Amino acid structures of residues involved in H2AX functions.

The interest in H2AX has only increased in recent years as its correlation with cancer has been identified. This histone is now the subject of research not only focused on its structure and function, but also on its possible utilization as a biomarker, as well as a therapeutic target [81]. Thus, H2AX has become more and more intriguing as a greater understanding of the unique properties of this histone variant have been elucidated.

γH2AX and DNA Double Strand Break Repair

In 1998 a molecular pharmacy lab at the NIH published one of the first papers to document the phosphorylation of H2AX after the induction of a DNA double strand break (DSB). In this study, DNA DSBs were induced into the chromatin of eukaryotic cells using various degrees of ionizing radiation exposure [78]. This study also showed that the time in which phosphorylated H2AX appears is as little as 20 seconds after DSB induction. Phosphorylated H2AX levels plateau at 10 minutes, and begin to decrease after 30 minutes. Later work from this same group [82] revealed that the phosphorylation of H2AX in the proximity of DNA DSBs is processive, that is, the phosphorylation of

H2AX initially occurs at the site of the DNA break and continues in both directions away from the break, forming a γH2AX locus extending up to a mega-base.

Through yeast knockout and mutation studies it was determined that the phosphorylation of the serine four residues from the carboxyl terminus in the conserved SQE motif (see above) is necessary for DNA DSB repair [3,79]. γH2AX facilitates DNA DSB repair in multiple pathways, although its importance varies amongst different species and pathways [2]. γH2AX is utilized, but is not essential, in processes in mammals such as non-homologous end joining (NHEJ) and homologous recombination (HR), likely due to functional redundancy with other proteins and the parallel evolution of pathways within more complex species [2]. However, in yeast many of these functions do require γH2AX and in all H2AX containing species γH2AX is essential for DNA replication [2]. Recent studies have also identified constitutively low levels of γH2AX in genomic regions without DSBs. The purpose of this low level γH2AX has been hypothesized to be in the recruitment of mitotic, silencing and replicative proteins, but as of yet is not fully understood [83].

The phosphatidylinositol-3-OH kinase-related kinases (PIKK) family of kinases are responsible for the phosphorylation of H2AX, and the correlation of PIKK mutations with DNA damage response diseases further illustrates the need for γH2AX in DNA double strand break repairs [6,7]. Both mammalian and yeast PIKKs share a common binding consensus sequence of Ser-Gln-Glu, once again linking them to the conserved SQE sequence of H2AX [3].

The elimination of γH2AX has been shown to correlate temporally with DSB repair completion [84]. Although still controversial, it is theorized that the

dephosphorylation of H2AX does not occur while the histone is bound to the nucleosome. Instead the FACT complex, which is known to incorporate H2A-H2B dimers into nucleosomes [85] is responsible for both incorporation and dissociation of H2AX-containing H2A-H2B dimers [86]. The FACT complex recognizes the specific phosphorylation of H2AX as a signal for histone removal [71]. Once γH2AX is removed from the nucleosome it is either dephosphorylated or targeted for degradation. Multiple phosphatases have been identified which dephosphorylate γH2AX, including protein phosphatase 1, protein phosphatase 2 and HTP-C, (the histone H2A phosphatase complex) [87,88].

The mechanisms by which γH2AX functions in DSB repair are, as yet, not fully understood. γH2AX has been identified to recruit and bind many DNA repair proteins and protein complexes. Some notable proteins which have been identified to co-localize to γH2AX are MDC1, Brca1, Rad51 and the Mre11-Rad50-Mbs1complex [7,12]. These proteins and protein complexes are all involved in either initiating or carrying out DNA break repair. The well characterized capability of γH2AX to recruit these repair factors has given rise to the theory that γH2AX's binding and recruitment of repair factors is the sole role of γH2AX in DNA double strand break repair. This pathway of protein binding and recruitment is supported by multiple pieces of evidence. First, kinetic studies of DNA repair foci have determined that the formation of γH2AX occurs before other factors assemble near the site of the break. Work from the Bonner lab utilizing fluorescently labeled antibodies mapped the formation and location of γH2AX, Rad50 and Brac1. This technique showed γH2AX initially forms a distinct foci at DNA DSBs, followed by an ordered recruitment of Rad50 and Brac1 [7].

Second, the presence of γH2AX is necessary for the recruitment repair factors [7]. This was shown by the same lab through the use of wortmannin, an inhibitor of H2AX phosphorylation in the same fluorescence assay. If the formation of γH2AX was blocked, neither Rad50 nor Brac1 localize to double strand break sites. Elledge and coworkers used a similar technique to elucidate the same relationship between γH2AX and MDC1 (Mediator of DNA damage checkpoint 1) [12]. Last, the phosphorylation of H2AX has been shown to create a novel binding site for DNA repair proteins. Immunoprecipitation assays preformed by the Elledge lab identified MDC1 as complexing with γH2AX but not H2AX suggesting that the phosphorylation leads to the formation of a distinct binding site [12].

The Nature of γH2AX Influence on Chromatin Secondary Structure

γH2AX has been thought to have the ability to alter chromatin condensation [3,80,89]. While phosphorylation of H2AX has been shown to recruit repair factors to the site of DSBs, it has also been postulated that this modification may loosen the chromatin near the break, thus allowing enhanced DNA access to the DNA repair machinery [3,80,89]. However, this result has been contradicted by other similar studies, and thus γH2AX has been demonstrated to affect and not affect the secondary structure of chromatin [3,10,11,90]. The addition of a phosphoryl group adds mass and negative charge to the CTD, and as this phosphorylation occurs on both copies of H2AX within a nucleosome, the possibility of steric or electrostatic interference between the histone dimers increases. It is also important to note that the addition of negative charge near the location at which the DNA enters and exits the nucleosome could lead to an electrostatic repulsion of the DNA and,

in theory, loosen the nucleosome. These changes may be further evidenced by changes in the ability of γH2AX-containing chromatin to form higher order structures, as is studied herein.

Taken together, the above literature (and inferences which can be drawn from them) leave in doubt the role of γH2AX in facilitating DSB repair. Specifically, it is unknown to what extent γH2AX-mediated DNA repair-associated protein recruitment versus chromatin architectural changes due to the presence of γH2AX contribute to the process as a whole. Thus, I have attempted to address this uncertainty by using a defined chromatin model system containing major-type-, H2AX- and γH2AX-containing octamers and studying the two salt-dependent, intrinsic chromatin transitions: folding and self-association. I hypothesize that γH2AX acts through a combination of repair factor recruitment and chromatin decondensation in aiding DNA DSB repair. Through these studies, I have demonstrated that both H2AX- and γH2AX-containing chromatin have a unique folding property, in that they are refractory to forming the maximally folded, 55 S structures, relative to the major-type H2A. All three types of chromatin self-associate identically, thus the difference appears to be specific to folding, and the implications of this difference with respect to DNA repair and the unique protein chemistry of H2AX are discussed.

Materials and Methods

601 207-12 Tandem-Repeat DNA Purification

The DNA for the defined nucleosome arrays was prepared as described [58]. Briefly, DH5α cells were transformed with pUC plasmid containing 207–12 DNA Simpson made this vector [91]. A glycerol stock of these cells was prepared, flash frozen and stored at -80 C. This stock was then streaked onto MacConkey agar plate with ampicillin and grown overnight at 37 °C. A colony was selected and grown in 5 ml LB medium containing ampicillin until cloudy and expanded to 6 liters before chloramphenicol was added. The culture was continued overnight until confluent. Cells were harvested and the plasmid was purified using a Qiagen Giga Prep (Valencia CA). The purified plasmid was digested with the restriction endonucleases XbaI, HindIII, DraI and HaeII, thus cutting the plasmid into seven fragments, the largest of which contains the 207-12 fragment (~2500bp). The digested DNA was purified on a Sephacryl S200 gel filtration column (15 mm x 115 cm) following an existing unpublished lab protocol; column was ran at a 0.4 mL/min flow rate with 50mM NaCl and fraction collection began after 4 hours. Fractions containing 207-12 fragment were collected, pooled, sodium acetate/ethanol precipitated and the re-solubilized DNA was stored at -20°C. Purity was confirmed by agarose gel electrophoresis.

Cloning of H2AX S135E

A pMA plasmid containing *Xenopus laevis* H2AX was obtained from GENEART (Burlingame CA). The plasmid was transformed intoTOP10 competent cells and

amplified. Polymerase chain reaction (PCR) primers were designed to both amplify the gene and to direct point mutagenesis of serine residue 135 to glutamic acid (AGC → GAA). The resulting S135E plasmid was transformed into top10 competent cells and amplified. Purification of the H2AX and H2AX S135E gene-encoding plasmids was performed using Qiagen mini prep kits, digested with NdeI and BamHI, gel-purified on 1.2% agarose, and extracted using the Qiagen QIAquick gel extraction kit. The amplified genes were ligated into pET3a plasmids (similarly digested with Nde1 and BamH1) using Roche Rapid DNA Ligation kit. pET3a plasmids (Novagen, EMD4Biosciences) containing H2AX and H2AX S135E were transformed into XL-1 Blue competent cells and amplified. The fidelity of the clones was determined by agarose electrophoresis of digestion products and DNA sequencing (Proteomics and Metabolomics Facility, Colorado State University).

Xenopus Core Histone Expression and Purification

BL21 DE3 pLysS cells were transformed with pET or pMA plasmids harboring the histone gene of interest. Histone expression, inclusion body isolation and protein purification were performed as described [92]. Analysis of the ion exchange and gel filtration column fractions was performed using SDS-PAGE. Purified histones were aliquoted, lyophilized and stored at -20°C until use.

Mass Spectrometry

H2AX and H2AX S135E proteins were analyzed for MW using MALDI-TOF mass spectrometry (Proteomics and Metabolomics Facility, CSU). Approximately1 µl of purified protein combined with 1 µl of 3,5-dimethoxy-4-hydroxycinnamic acid (sinapinic acid, 10 mg/ml in 50% ACN, 0.1% TFA) was dropped on the MALDI target and air

dried. Sample analysis was preformed by an Ultraflex-TOF/TOF mass spectrometer (Bruker Daltonics, Billerica, MA) in positive ion, linear mode, 25 kV accelerating voltage. A protein calibration mixture (4 to 6 proteins) was used as a control spotted next to the H2AX and H2AX S135E proteins. Data was processed using FlexAnalysis software (version 2.4, Bruker Daltonics).

Histone Octamer Assembly and Purification

Lyophilized histones were dissolved in denaturation buffer and adjusted to a concentration of 1mg/ml essentially as described [93]. Briefly, equimolar amounts of each histone were mixed together to produce the correct stoichiometric structure in octamer refolding (1:1:1:1 of H2A:H2B:H3:H4). Histones were transferred to Spectra-Por dialysis tubing (6-8 kDa) and dialyzed with three sequential changes of refolding buffer to remove urea and exchange into 2M NaCl. The assembled octamers were concentrated to 1.5–2.0 ml (~ 10 mg/ml) and purified via Superdex S-200 (GE Healthcare) (16mm x 60cm) gel filtration. The purity of collected octamer fractions was determined with SDS-PAGE. Pooled, refolded octamer fractions were stored at 4 °C until needed for nucleosome array reconstitution.

Reconstitution of Nucleosomal Arrays

Nucleosomal arrays were reconstituted using 207–12 DNA and purified core histone octamers as described previously [94]. Briefly, the octamer/DNA mixtures were dialyzed stepwise against decreasing concentrations of salt from 2M to 2.5mM. Reconstituted nucleosomal arrays were stored at 4 °C until needed.

Sedimentation Velocity

The degree of saturation (number of octamers per template) of the nucleosome array was determined by sedimentation velocity in TEN buffer performed using a Beckman XLA or XLI analytical ultracentrifuge with UV scanner optics as described previously [95]. The van Holde and Weischet method was used to analyze scans [96]. Ultrascan data analysis software was utilized to determine the diffusion corrected, integral distribution of sedimentation coefficients [G(s) distributions (Dr. B. Demeler, University of Texas Health Science Center, San Antonio, TX)]. The mean sedimentation coefficient (s_{mid}) was determined as the sedimentation coefficient at boundary fraction = 0.5.

Self Association Assay

Self Associations were carried out as previously described [48,58]. Briefly, nucleosome arrays were brought to an $O.D._{260}$ of 1.0 with TEN buffer (10 mM Tris pH 7.8, 0.25 mM EDTA, 2.5 mM NaCl). Equal amount of array and MgCl2–TEN buffer ([MgCl2] of 0-3.25 mM) were mixed, incubated for 5 min at ~22 ºC and centrifuged for 5 minutes at 13,000 rpm (16,000×g). The supernatant was then removed and placed in a Beckman DU 800 Spectrophotometer where the Abs260nm was recorded. The percentage of sample that remained in solution was plotted against the concentration of $MgCl_2$ to generate a self-association plot.

Results

The ability of γH2AX to alter the condensation of chromatin remains unclear. To date, all studies that have speculated on this property have been performed *in vivo* [3,10,11,90]. To directly determine if H2AX or γH2AX affects the ability of chromatin to form higher order structures, we used *in vitro* assays taking advantage of a well characterized, defined length nucleosome array model system that has previously been shown to accurately identify the structural effects of histone modifications and mutations on chromatin [12,36,38,55,97]. Octamers containing H2A, H2AX and the phosphor-mimic of γH2AX (S36E) were compared through these assays to determine what, if any, structural affects these histone variants exert on the chromatin fiber. Substitution of serine with a glutamic acid has previously been shown to imitate γH2AX in *in vivo* assays, due to its similar van der Waals radius and charge distribution [3,10,79]. Using H2A-, H2AX- and H2AX S135E-containing octamers, homogenously saturated nucleosomal arrays were reconstituted onto the 601 DNA. Folding and self association assays carried out with these nucleosomal arrays identified key structural similarities and functional differences between the H2A variants.

Reconstituting Homogenously Saturated Nucleosomal Arrays

601 DNA [50] was used for nucleosome array reconstitution to achieve optimal nucleosome positioning and homogenous template saturation. This DNA is a 2500 base pair long fragment of linear DNA containing 12 repeats of the 601 sequence which is 207 base pairs in length. The 601 nucleotide sequence has been selected for and determined

to have high nucleosomal binding affinity, and centrally positions one nucleosome per 207bp repeat [50]. Nucleosomal array saturation and homogeneity were determined using sedimentation velocity in low salt conditions (TEN). Homogeneity of nucleosomal array stocks is essential to allow direct comparison between condensation properties of each of the histone variants. Folding and self-association assays are sensitive to the saturation of the template; templates with more nucleosomes are more readily folded and self-associated [28]. Arrays were reconstituted to full 12-mer saturation with an approximate sedimentation coefficient of 29S as seen in figure 5A [98,99]. More specifically, 50% or more of the H2A- and H2AX-containing nucleosomal arrays and 30% or more of the H2AX S135E arrays were at full saturation. Less than 10% of each array was sub-saturated, meaning under 11-mer saturation (~26.6S). The saturation of all three arrays was highly comparable with approximately one-half nucleosome difference, suggesting very high homogeneity and similarity. Thus any dissimilarity in folding or self association of these assays can be directly contributed to the differences between the histone variants, rather than difference in template saturation.

H2A, H2AX and H2AX S135E Fold to the Moderately Folded Material (40S) Comparably, but Vary in Their Ability to Form the Maximally Folded (30nm) Species.

Homogenously saturated arrays containing H2A, H2AX and H2AX S135E were assayed for folding in 0.25 mM- 1.25 mM $MgCl_2$. At low salt concentrations (0.25-0.5 mM $MgCl_2$) nucleosome arrays typically fold to form a mixture of unfolded and intermediately folded structures [28]. Under these same ionic conditions, all three of the arrays tested here form intermediately folded structures identically, as seen in figure 5B and 5C. At 0.25 mM $MgCl_2$ approximately 15% or less of the material in all

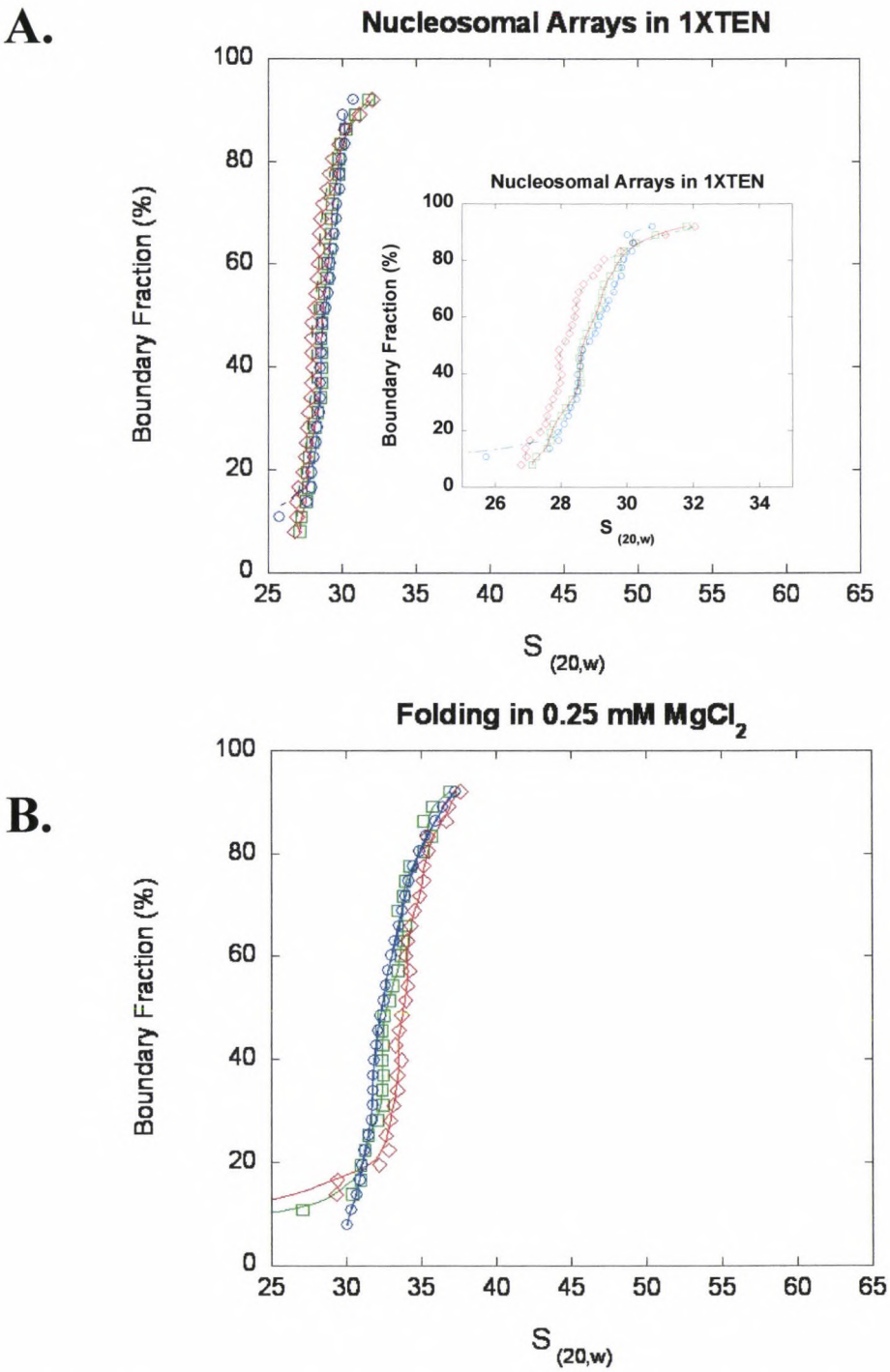

Figure 5 G(s) distributions from sedimentation velocity data from typical, nearly saturated nucleosomal arrays used in this study. H2A (□), H2AX (○) and H2AX S135E (◇). A) Arrays in 1X TEN B) Arrays in 0.25 mM $MgCl_2$ C) Arrays in 0.5 mM $MgCl_2$ D) Arrays in 0.75 mM $MgCl_2$ E) Arrays in 1.0 mM $MgCl_2$ F) Arrays in 1.25 mM $MgCl_2$

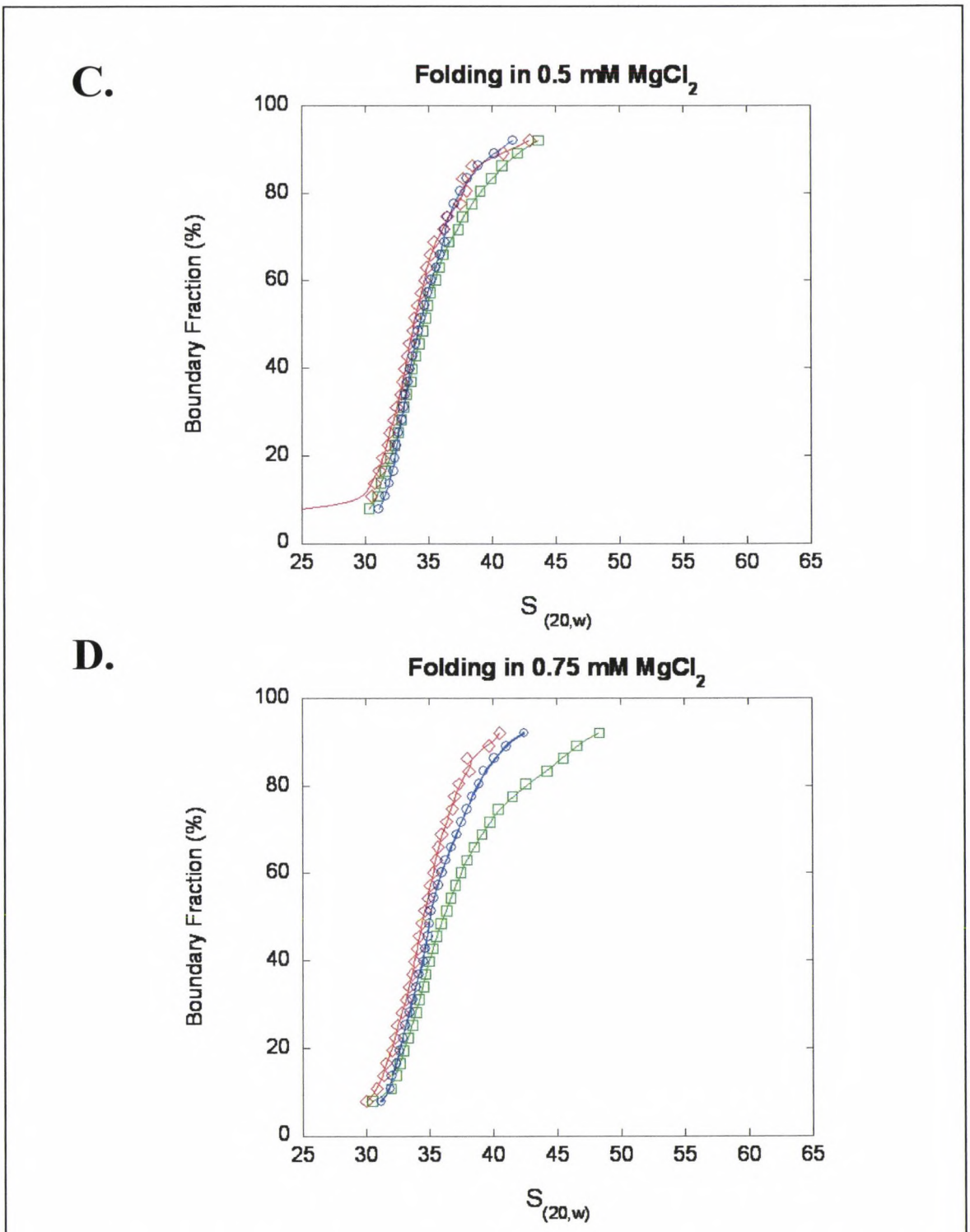

Figure 5 G(s) distributions from sedimentation velocity data from typical, nearly saturated nucleosomal arrays used in this study. H2A (□), H2AX (○) and H2AX S135E (◇). A) Arrays in 1X TEN B) Arrays in 0.25 mM $MgCl_2$ C) Arrays in 0.5 mM $MgCl_2$ D) Arrays in 0.75 mM $MgCl_2$ E) Arrays in 1.0 mM $MgCl_2$ F) Arrays in 1.25 mM $MgCl_2$

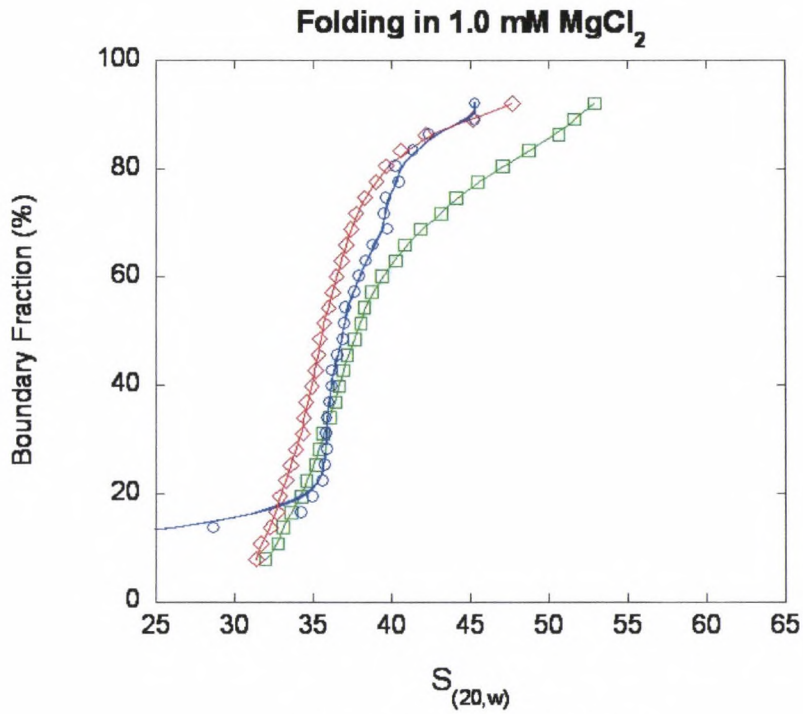

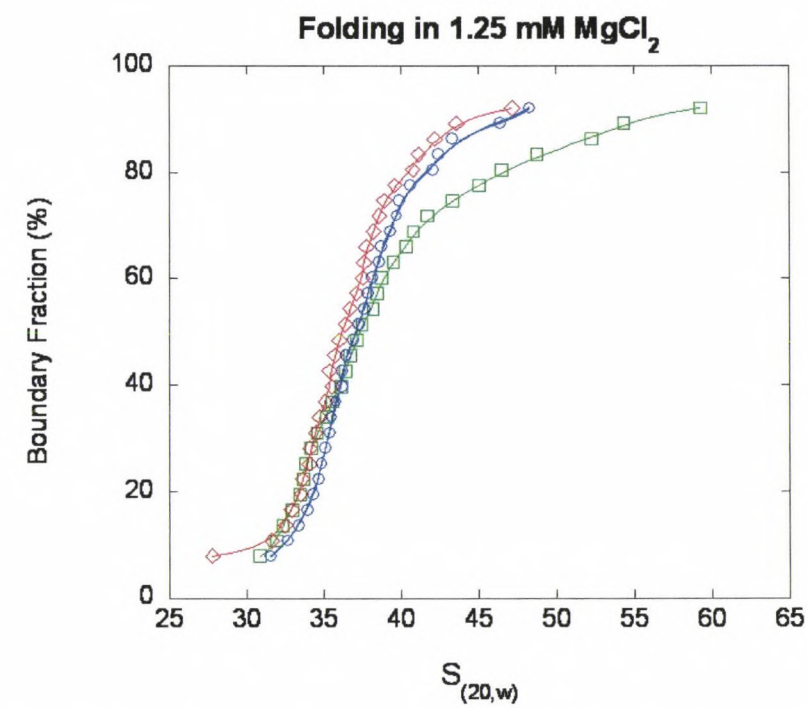

Figure 5 G(s) distributions from sedimentation velocity data from typical, nearly saturated nucleosomal arrays used in this study. H2A (□), H2AX (○) and H2AX S135E (◇). A) Arrays in 1X TEN B) Arrays in 0.25 mM $MgCl_2$ C) Arrays in 0.5 mM $MgCl_2$ D) Arrays in 0.75 mM $MgCl_2$ E) Arrays in 1.0 mM $MgCl_2$ F) Arrays in 1.25 mM $MgCl_2$

three arrays is less than 30S (unfolded), ~65% is 30S-35S (slightly folded) and the remaining 20% is intermediately folded, with a sedimentation coefficient between 35 and 40S. Folding of the three arrays remained similar at 0.5 mM $MgCl_2$ with less than 5% under 30S, 55% between 30S and 35S and the remaining 40% between and 35 and 45 S.

Maximally folded material, commonly referred to as the 30nm fiber, occurs through further intra-nucleosomal interactions. This compaction begins to occur in H2A-containing arrays in 0.75 mM $MgCl_2$ and is even more prevalent with increasing $MgCl_2$ concentration. However, neither the H2AX nor H2AX S135E arrays begin to form 55S material in 0.75-1.25 mM $MgCl_2$. Specifically at 0.75 mM $MgCl_2$ all three arrays have 40% of their material sedimenting between 30S and 35S. The remaining 50% of H2AX and H2AX S135E is relatively equally divided between 35S and 40S with the remaining 10% reaching approximately 42S. However, H2A forms much more folded material at this ionic strength, reaching 49S with a less homogenous distribution. In 1.0 mM $MgCl_2$ this trend is further exaggerated with 80% H2AX and H2AX S135E evenly distributed between 30S and 40S with the last 20% approaching 47S. H2A shows a distribution, with 55% of its arrays between 30s and 40S, while the upper 45% becomes increasingly heterogeneous, ultimately reaching a maximally folded confirmation at ~55S. 1.25 mM $MgCl_2$ shows a continuation of H2A maximal folding with 10% of the material at or above 55S, 35% unevenly distributed between 40s and 55S and the last 55% still evenly sedimenting between 30S and 40S. H2AX and H2AX S135E reach a maximum sedimentation of approximately 47S with 80% of the material sedimenting between 30S and 40S at this same $MgCl_2$ concentration. This difference in their ability to form the 55S structure(s) can be directly correlated to the H2A variant within the arrays, since this is

the only variable between the three arrays. Collectively this data suggests that H2AX and H2AX S135E arrays are refractory to the formation of 55S material relative to wild type arrays.

H2A, H2AX and H2AX S139E Oligomerize Analogously

Identically saturated nucleosomal arrays containing the three H2A variants were subjected to self-association assays using $MgCl_2$ concentrations of 0 mM to 3.25 mM. Oligomerization was determined using spectrophotometric analysis of the supernatant after low speed sedimentation had pelleted out any oligomerized material from the sample. The normalized absorbance, which is determined to be the percent of array not self associated, is plotted against $MgCl_2$ concentration to produce a self association curve [56]. Typical self-association profiles for nucleosome arrays are shown in figure 6. All three arrays show the classic self-association plot profile, where, after a brief lag phase at $MgCl_2 < 1.0$mM (the same salt conditions which led to intermediate and maximal folding [see above]), the arrays remain largely soluble until ~1.5mM $MgCl_2$, at which point they demonstrate a highly cooperative self-association transition. At ~2.5 mM $MgCl_2$, most of the nucleosome array has self-associated and is in the pellet. Figure 6 also shows a high level of similarity between the oligomerization profiles of all three H2A variants. The Mg_{50} (that is, the $MgCl_2$ concentration at which 50% of the sample has oligomerized), is often used to compare characterize self association profiles [28,57,58]. The Mg_{50}s of the three arrays show no statistically significant differences (Fig, 6 B). The shape of the oligomerization profiles also shows that this process is similarly cooperative for all three variants. Together, these results indicate that nucleosome arrays containing H2A, H2AX and H2AX S135E appear to behave identically with regards to their abilities to

oligomerize, suggesting a specificity regarding the differences seen in the above-described folding assays.

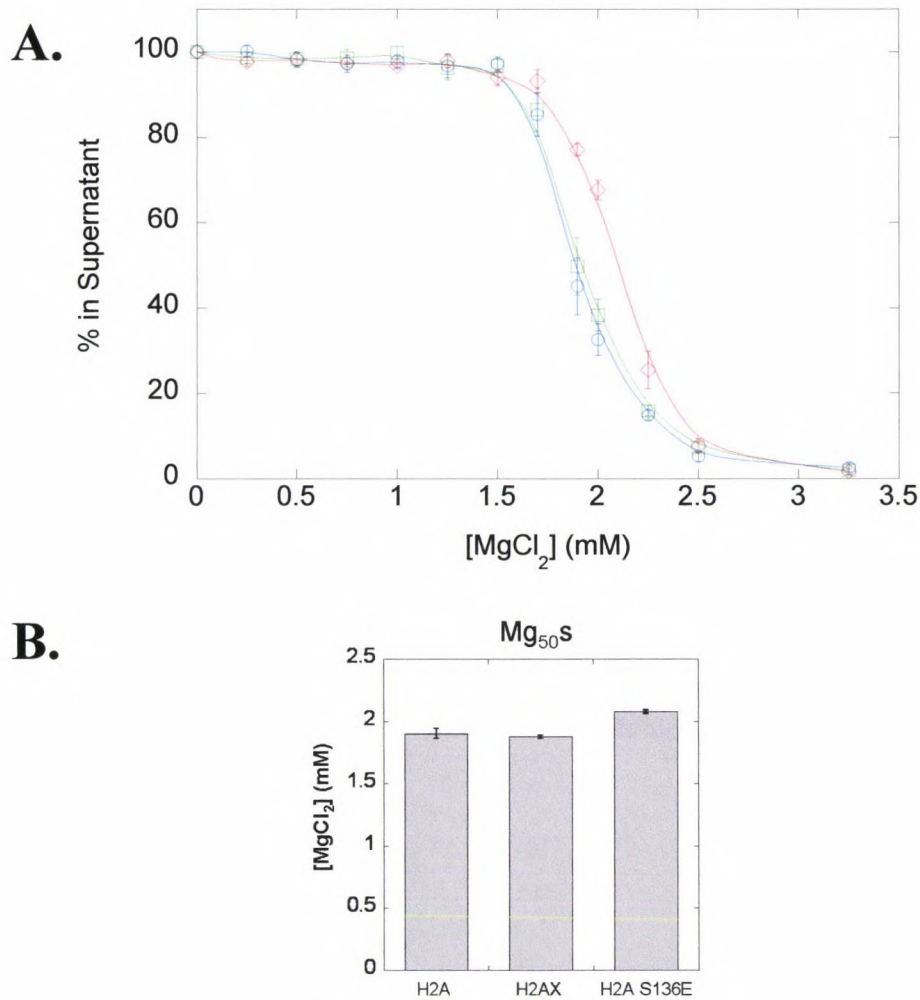

Figure 6 Self Association plots of H2A- (□), H2AX- (○) and H2AX S135E-containing (◇) nucleosomal arrays. (A) Percent remaining in the supernatant (soluble) as a function of [$MgCl_2$]. (B) Mg_{50} values were determined from self-association data. Error bars represent the standard deviation from 2-4 independent self association assays.

Discussion

Although H2AX and its phosphorylated form have been the center of much research, the role of this H2A variant on chromatin condensation remained controversial in the scientific literature. The research described in this thesis has provided direct data in support of a role for H2AX and γH2AX in chromatin condensation. Importantly, these results come from a highly pure, homogenous and controlled *in vitro* system which allows the results to clearly relate both folding and self association changes directly to the influence of the H2A variants. The results of these experiments have demonstrated that the presence of either H2AX or γH2AX within a nucleosome has the ability to alter the folding, but not the oligomerization, properties of the chromatin fiber.

Folding assays demonstrate that H2A, H2AX and γH2AX have nearly identical folding in low salt, but begin to differentiate from one another as they adopt a conformation that leads to the observation of the >40S species. Specifically, incubation of these arrays in low concentrations of salt (0.25-0.5 mM MgCl2) shows similar folding between all three H2A variants with regards to the formation of 40S species (Fig. 5B-C). This data illustrates that arrays containing H2AX and γH2AX are capable of forming the interactions required for intermediately folded species similar to arrays containing major-type H2A. Similarities between the arrays are lost when they are incubated in higher concentrations of salt (0.75-1.0 mM MgCl2) (Fig. 5D-E). Under these conditions, H2A-containing arrays become increasingly more folded, meeting and exceeding the 55S threshold for maximum folding, while both the H2AX and γH2AX are much less prone

to forming the 55S structures. At 1.25 mM MgCl2 this difference is more distinct, with approximately 10% of the H2A arrays folding into 55S or greater material, while the H2AX and γH2AX arrays fail to fold beyond 50S (Fig. 5F).

The difference in folding between H2A and H2AX/γH2AX containing arrays may be due to either: 1) the length variation in the CTDs, 2) the amino acid variation in the CTDs, and/or 3) the minor amino acid substitutions within the globular domain. These first two possibilities focus on residues that are positioned to exit the nucleosome at the dyad axis, and thus have a multitude of potential influences on the chromatin fiber. Perhaps there is an alteration in the exact position near the dyad axis at which the H2A tails protrude when H2AX/γH2AX is present, and this may alter the path or extent of DNA wrapping. Thus, when H2AX/γH2AX histones are present this condensation pathway is inhibited. Altering the length or physico-chemical properties of the CTD at the dyad axis may affect : a) the stability of the octamer within the nucleosome, b) the accessibility of the linker DNA, and c) direct interactions or create steric clashes with adjacent core histone NTDs. The length variation of the H2AX/γH2AX CTD may be capable of all three of these effects. The CTD of H2AX/γH2AX histones are ~ 9 amino acids longer than that of the major-type H2A. The 18 additional residues (9 from each H2AX/γH2AX copy) may preclude the DNA from being able to wrap the octamer tightly or affect the ability of the nucleosome to slide to accommodate the formation of the 30nm fiber. Similarly, when the amino acid composition is taken into account, the ability of H2AX/γH2AX to interfere with the dyad axis during folding becomes more apparent. The CTD of major type H2A is made up of 13 amino acid residues and lacks any structured regions, making it highly flexible. On the other hand, the H2AX CTD

A.

	# of Res.	Lys *D*	Pro *D*	Gly *D*	Arg *D*	Asn *D*	Gln *D*	Ser *D*	Glu *D*	Asp *D*	Met *D*	Ala *N*	Thr *N*	Val *O*	His *O*	Phe *O*	Ile *O*	Leu *O*	Cys *O*	Trp *O*	Tyr *O*
H2A CTD	13	38.5	7.7	0	0	0	0	30.8	7.7	0	0	0	15.4	0	0	0	0	0	0	0	0
H2AX CTD	22	18.2	4.5	13.6	0	0	13.6	31.8	4.5	0	0	0	4.5	4.5	0	0	0	0	0	0	4.5
H2A	129	10.1	3.9	10.9	9.3	4.7	3.9	5.4	5.4	1.6	0	12.4	4.7	7	1.6	0.8	3.9	12.4	0	0	2.3
H2AX	138	8.7	3.6	10.9	8.7	4.3	5.1	8.7	4.3	1.4	0	11.6	3.6	8	2.2	0.7	3.6	11.6	0	0	2.9

B.

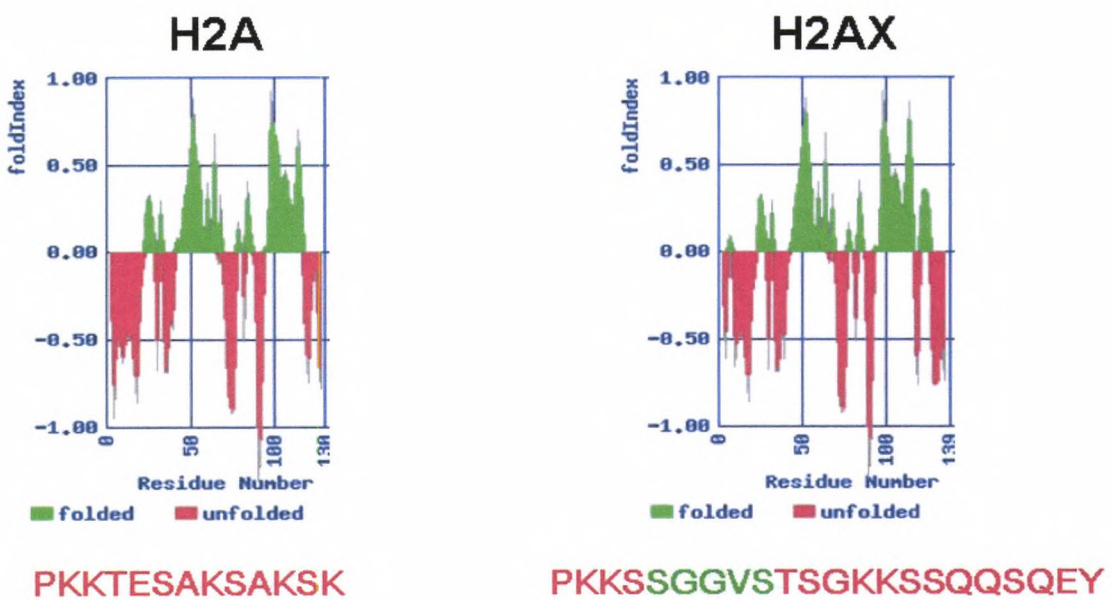

Figure 7. Amino acid composition (A) and secondary structure predictions (B) for the *Xenopus laevis* H2A and H2AX CTDs. (A) Amino acid side chains are categorized into D (disorder-producing); N (neutral), and O (order-producing). (B) FoldIndex plots of the full-length H2A and H2AX proteins. Below amino acid sequence of CTDs color coded for folded (green) versus unfolded (red). Created using FoldIndex© [1]

contains two amino acids, a valine and a tyrosine, known to contribute to protein secondary structure (Fig. 7). Using Fold Index [1] plot analysis, a powerful and highly accurate predictor of disorder within proteins and peptides, H2AX is shown to have a 5 residue region of predicted structure between residues 121-125 within the CTD. This structured region may alter the typically compliant nature of the tail, and thus alter either the stability of the octamer within the nucleosomal DNA, the accessibility of the linker DNA and/or the interactions with adjacent core histone NTDs. This, in turn, could lead to a reduction in 30nm fiber formation

Lastly, the globular regions of H2A and H2AX also vary at a key residue which has been shown to be involved in binding between the two H2A-H2B dimers across the octamer, as mentioned previously. The 42nd residue is a glutamic acid in H2A, but a histidine in H2AX. The switch from glutamic acid to histidine directly would displace a hydrogen bond that forms between the two H2As within the histone octamer [18], and therefore could result in a weaker H2A-H2A intra-octamer interaction. Altering the intra-nucleosomal bonds could decrease the ability of the array to undergo compaction and/or increase nucleosome flexing. A recent study using human H2AX, which has a disruption in this bond due to similar a amino acid substitution, identified a decrease in the stability of nucleosomes containing H2AX, relative to H2A [80]. This nucleosome destabilization may alter chromatin condensation pathways.

The data from self association assays did not identify any significant differences between the nucleosomal arrays tested in this study. This result is not surprising, since self association/oligomerization is a process involving a great number of macromolecular interactions occurring between many individual NTDs. Importantly, it has been shown

that all four core histone NTDs contribute additively and independently to self-association [58], and that the NTDs can be swapped (as long as the length and surface charge densities remain constant) without affecting self-association. The specific steric hindrance (CTD length and secondary structure) or intra-nucleosomal bond alteration that may be influencing maximal folding are not deleterious enough to reduce the numerous cis- and trans-interactions that take place during oligomerization. The fact that oligomerization occurs between different arrays may reduce any impact of H2AX/γH2AX, because compaction at the dyad axis may not be as much of a requisite for inter-nucleosome interactions as it is for intra- nucleosome interactions.

Close inspection of the folding profiles also reveals that, in general, the H2AX S135E containing arrays lag slightly behind the H2AX-containing arrays. This suggests that phosphorylation of H2AX may have a slight affect on chromatin condensation. The H2AX arrays fold to a slightly lesser extent, signifying that the addition of a charge group to the CTD may increase the inhibitory affect that H2AX has on close range, intra-nucleosomal compaction. However, it must be noted that this lag may correlate to the slight difference in the saturation of the arrays. At close inspection the H2AX S135E array may have a higher portion of arrays that are 11-mers than the H2AX array stock. Having a lower number of octamers per DNA template may cause a shift in folding as seen in the comparison of H2AX S135E to H2AX. In any case, this difference in folding is small relative to the difference between H2A and H2AX, indicating that the addition of ~3 negative charges at the carboxyl-terminal end of the CTD does not globally influence chromatin dynamics. This modification must, as suggested elsewhere, create or alter a binding site for proteins involved in DNA double strand break repair.

H2AX's biological relevance to DNA DSB repair may help place these results in context. H2AX is suggested to be randomly dispersed throughout the genome, thus act to readily signal damage and summon DNA DSB repair proteins when phosphorylated. The presence of H2AX itself inhibits maximal folding but not moderate folding or self association, thus these states may provide a chromatin environment that tolerates rapid dynamics necessary for DNA repair, while reducing the highest level of folding. Reduction in maximally folded chromatin may allow repair factors or chromatin remodelers better and more local access to damaged regions. This reduction in maximal folding was shown to be present in arrays containing both H2AX and H2AX S135E. Thus, it appears that γH2AX's role in DNA double strand break repair is, at least in part, to signal the site of the break and recruit repair factors, not to globally decondense chromatin.

Recent work published from Juan Ausio's lab has suggested that the phosphorylation of H2AX may play a key role in chromatin decondensation in an indirect manner, its relationship with linker histone, H1 [80]. The CTD of H2AX is known to contact the globular domain of the linker histone H1 bound to the linker DNA [67]. Dr Ausio's work suggests that when H2AX is phosphorylated the binding of H1 to chromatin is reduced. Furthermore, when both H2AX and H1 are phosphorylated the binding of H1 is almost completely inhibited [80]. This H2AX-H1 relationship may be the reason that past *in vivo* studies have seen a marked relaxation in chromatin structure in the presence of γH2AX, as the loss of H1 would certainly have a profound influence on the chromatin fiber. It will be of paramount importance to continue investigation into this mechanism using the system of *in vitro* assays detailed in this study, to attempt to

better understand the dynamic role of H2AX and H1 in chromatin condensation and DNA DSB identification and repair.

References

1. Prilusky, J. et al. FoldIndex: a simple tool to predict whether a given protein sequence is intrinsically unfolded. *Bioinformatics* **21**, 3435-8 (2005).
2. Fernandez-Capetillo, O., Lee, A., Nussenzweig, M. & Nussenzweig, A. H2AX: the histone guardian of the genome. *DNA Repair (Amst)* **3**, 959-67 (2004).
3. Downs, J. A., Lowndes, N. F. & Jackson, S. P. A role for Saccharomyces cerevisiae histone H2A in DNA repair. *Nature* **408**, 1001-4 (2000).
4. Chen, H. T. et al. Response to RAG-mediated VDJ cleavage by NBS1 and gamma-H2AX. *Science* **290**, 1962-5 (2000).
5. Fernandez-Capetillo, O. et al. H2AX is required for chromatin remodeling and inactivation of sex chromosomes in male mouse meiosis. *Dev Cell* **4**, 497-508 (2003).
6. Durocher, D. & Jackson, S. P. DNA-PK, ATM and ATR as sensors of DNA damage: variations on a theme? *Curr Opin Cell Biol* **13**, 225-31 (2001).
7. Paull, T. T. et al. A critical role for histone H2AX in recruitment of repair factors to nuclear foci after DNA damage. *Curr Biol* **10**, 886-95 (2000).
8. Ward, I. M. & Chen, J. Histone H2AX is phosphorylated in an ATR-dependent manner in response to replicational stress. *J Biol Chem* **276**, 47759-62 (2001).
9. Burma, S., Chen, B. P., Murphy, M., Kurimasa, A. & Chen, D. J. ATM phosphorylates histone H2AX in response to DNA double-strand breaks. *J Biol Chem* **276**, 42462-7 (2001).
10. Fink, M., Imholz, D. & Thoma, F. Contribution of the serine 129 of histone H2A to chromatin structure. *Mol Cell Biol* **27**, 3589-600 (2007).
11. Kruhlak, M. J. et al. Changes in chromatin structure and mobility in living cells at sites of DNA double-strand breaks. *J Cell Biol* **172**, 823-34 (2006).
12. Stewart, G. S., Wang, B., Bignell, C. R., Taylor, A. M. & Elledge, S. J. MDC1 is a mediator of the mammalian DNA damage checkpoint. *Nature* **421**, 961-6 (2003).
13. Luger, K. & Hansen, J. C. Nucleosome and chromatin fiber dynamics. *Curr Opin Struct Biol* **15**, 188-96 (2005).
14. Hansen, J. C. Conformational dynamics of the chromatin fiber in solution: determinants, mechanisms, and functions. *Annu Rev Biophys Biomol Struct* **31**, 361-92 (2002).
15. Zlatanova, J., Bishop, T. C., Victor, J. M., Jackson, V. & van Holde, K. The nucleosome family: dynamic and growing. *Structure* **17**, 160-71 (2009).
16. Wachsmuth, M., Caudron-Herger, M. & Rippe, K. Genome organization: balancing stability and plasticity. *Biochim Biophys Acta* **1783**, 2061-79 (2008).
17. Arents, G., Burlingame, R. W., Wang, B. C., Love, W. E. & Moudrianakis, E. N. The nucleosomal core histone octamer at 3.1 A resolution: a tripartite protein

assembly and a left-handed superhelix. *Proc Natl Acad Sci U S A* **88**, 10148-52 (1991).
18. Luger, K., Mader, A. W., Richmond, R. K., Sargent, D. F. & Richmond, T. J. Crystal structure of the nucleosome core particle at 2.8 A resolution. *Nature* **389**, 251-60 (1997).
19. Felsenfeld, G. & Groudine, M. Controlling the double helix. *Nature* **421**, 448-53 (2003).
20. Wu, C., Bassett, A. & Travers, A. A variable topology for the 30-nm chromatin fibre. *EMBO Rep* **8**, 1129-34 (2007).
21. Arents, G. & Moudrianakis, E. N. The histone fold: a ubiquitous architectural motif utilized in DNA compaction and protein dimerization. *Proc Natl Acad Sci U S A* **92**, 11170-4 (1995).
22. Luger, K. & Richmond, T. J. The histone tails of the nucleosome. *Curr Opin Genet Dev* **8**, 140-6 (1998).
23. Lee, D. Y., Hayes, J. J., Pruss, D. & Wolffe, A. P. A positive role for histone acetylation in transcription factor access to nucleosomal DNA. *Cell* **72**, 73-84 (1993).
24. Ausio, J., Dong, F. & van Holde, K. E. Use of selectively trypsinized nucleosome core particles to analyze the role of the histone "tails" in the stabilization of the nucleosome. *J Mol Biol* **206**, 451-63 (1989).
25. Hecht, A., Laroche, T., Strahl-Bolsinger, S., Gasser, S. M. & Grunstein, M. Histone H3 and H4 N-termini interact with SIR3 and SIR4 proteins: a molecular model for the formation of heterochromatin in yeast. *Cell* **80**, 583-92 (1995).
26. Georgel, P. T., Tsukiyama, T. & Wu, C. Role of histone tails in nucleosome remodeling by Drosophila NURF. *Embo J* **16**, 4717-26 (1997).
27. Lee, K. M. & Hayes, J. J. Linker DNA and H1-dependent reorganization of histone-DNA interactions within the nucleosome. *Biochemistry* **37**, 8622-8 (1998).
28. Fletcher, T. M. & Hansen, J. C. The nucleosomal array: structure/function relationships. *Crit Rev Eukaryot Gene Expr* **6**, 149-88 (1996).
29. Hansen, J. C. Linking genome structure and function through specific histone acetylation. *ACS Chem Biol* **1**, 69-72 (2006).
30. Fischle, W., Wang, Y. & Allis, C. D. Histone and chromatin cross-talk. *Curr Opin Cell Biol* **15**, 172-83 (2003).
31. Peterson, C. L. & Laniel, M. A. Histones and histone modifications. *Curr Biol* **14**, R546-51 (2004).
32. Aaronson, R. P. & Woo, E. Organization in the cell nucleus: divalent cations modulate the distribution of condensed and diffuse chromatin. *J Cell Biol* **90**, 181-6 (1981).
33. Olins, D. E. & Olins, A. L. Physical studies of isolated eucaryotic nuclei. *J Cell Biol* **53**, 715-36 (1972).
34. Weith, A. Mg2+-dependent compactness of heterochromatic chromosome segments. *Exp Cell Res* **146**, 199-203 (1983).
35. Butler, P. J. & Thomas, J. O. Changes in chromatin folding in solution. *J Mol Biol* **140**, 505-29 (1980).

36. Belmont, A. S., Braunfeld, M. B., Sedat, J. W. & Agard, D. A. Large-scale chromatin structural domains within mitotic and interphase chromosomes in vivo and in vitro. *Chromosoma* **98**, 129-43 (1989).
37. Belmont, A. S. & Bruce, K. Visualization of G1 chromosomes: a folded, twisted, supercoiled chromonema model of interphase chromatid structure. *J Cell Biol* **127**, 287-302 (1994).
38. Schalch, T., Duda, S., Sargent, D. F. & Richmond, T. J. X-ray structure of a tetranucleosome and its implications for the chromatin fibre. *Nature* **436**, 138-41 (2005).
39. Dorigo, B., Schalch, T., Bystricky, K. & Richmond, T. J. Chromatin fiber folding: requirement for the histone H4 N-terminal tail. *J Mol Biol* **327**, 85-96 (2003).
40. Dorigo, B. et al. Nucleosome arrays reveal the two-start organization of the chromatin fiber. *Science* **306**, 1571-3 (2004).
41. Fan, J. Y., Rangasamy, D., Luger, K. & Tremethick, D. J. H2A.Z alters the nucleosome surface to promote HP1alpha-mediated chromatin fiber folding. *Mol Cell* **16**, 655-61 (2004).
42. Kan, P. Y., Lu, X., Hansen, J. C. & Hayes, J. J. The H3 tail domain participates in multiple interactions during folding and self-association of nucleosome arrays. *Mol Cell Biol* **27**, 2084-91 (2007).
43. Kan, P. Y., Caterino, T. L. & Hayes, J. J. The H4 tail domain participates in intra- and internucleosome interactions with protein and DNA during folding and oligomerization of nucleosome arrays. *Mol Cell Biol* **29**, 538-46 (2009).
44. Woodcock, C. L. Chromatin architecture. *Curr Opin Struct Biol* **16**, 213-20 (2006).
45. Widom, J. Chromatin structure: linking structure to function with histone H1. *Curr Biol* **8**, R788-91 (1998).
46. McBryant, S. J., Adams, V. H. & Hansen, J. C. Chromatin architectural proteins. *Chromosome Res* **14**, 39-51 (2006).
47. Reeves, R. Nuclear functions of the HMG proteins. *Biochim Biophys Acta* **1799**, 3-14.
48. Lu, X., Klonoski, J. M., Resch, M. G. & Hansen, J. C. In vitro chromatin self-association and its relevance to genome architecture. *Biochem Cell Biol* **84**, 411-7 (2006).
49. Simpson, R. T., Thoma, F. & Brubaker, J. M. Chromatin reconstituted from tandemly repeated cloned DNA fragments and core histones: a model system for study of higher order structure. *Cell* **42**, 799-808 (1985).
50. Lowary, P. T. & Widom, J. New DNA sequence rules for high affinity binding to histone octamer and sequence-directed nucleosome positioning. *J Mol Biol* **276**, 19-42 (1998).
51. Bednar, J., Horowitz, R. A., Dubochet, J. & Woodcock, C. L. Chromatin conformation and salt-induced compaction: three-dimensional structural information from cryoelectron microscopy. *J Cell Biol* **131**, 1365-76 (1995).
52. Hansen, J. C. & Turgeon, C. L. Analytical ultracentrifugation of chromatin. *Methods Mol Biol* **119**, 127-41 (1999).
53. Ausio, J. Analytical ultracentrifugation and the characterization of chromatin structure. *Biophys Chem* **86**, 141-53 (2000).

54. Hansen, J. C., Ausio, J., Stanik, V. H. & van Holde, K. E. Homogeneous reconstituted oligonucleosomes, evidence for salt-dependent folding in the absence of histone H1. *Biochemistry* **28**, 9129-36 (1989).
55. Schwarz, P. M. & Hansen, J. C. Formation and stability of higher order chromatin structures. Contributions of the histone octamer. *J Biol Chem* **269**, 16284-9 (1994).
56. Schwarz, P. M., Felthauser, A., Fletcher, T. M. & Hansen, J. C. Reversible oligonucleosome self-association: dependence on divalent cations and core histone tail domains. *Biochemistry* **35**, 4009-15 (1996).
57. McBryant, S. J. et al. Determinants of histone H4 N-terminal domain function during nucleosomal array oligomerization: roles of amino acid sequence, domain length, and charge density. *J Biol Chem* **284**, 16716-22 (2009).
58. Gordon, F., Luger, K. & Hansen, J. C. The core histone N-terminal tail domains function independently and additively during salt-dependent oligomerization of nucleosomal arrays. *J Biol Chem* **280**, 33701-6 (2005).
59. Kouzarides, T. Chromatin modifications and their function. *Cell* **128**, 693-705 (2007).
60. Doenecke, D. & Gallwitz, D. Acetylation of histones in nucleosomes. *Mol Cell Biochem* **44**, 113-28 (1982).
61. DeLange, R. J. & Smith, E. L. Histones: structure and function. *Annu Rev Biochem* **40**, 279-314 (1971).
62. Bradbury, E. M. Reversible histone modifications and the chromosome cell cycle. *Bioessays* **14**, 9-16 (1992).
63. Nathan, D., Sterner, D. E. & Berger, S. L. Histone modifications: Now summoning sumoylation. *Proc Natl Acad Sci U S A* **100**, 13118-20 (2003).
64. Fukuda, H., Sano, N., Muto, S. & Horikoshi, M. Simple histone acetylation plays a complex role in the regulation of gene expression. *Brief Funct Genomic Proteomic* **5**, 190-208 (2006).
65. Shogren-Knaak, M. et al. Histone H4-K16 acetylation controls chromatin structure and protein interactions. *Science* **311**, 844-7 (2006).
66. Shogren-Knaak, M. & Peterson, C. L. Switching on chromatin: mechanistic role of histone H4-K16 acetylation. *Cell Cycle* **5**, 1361-5 (2006).
67. Usachenko, S. I., Bavykin, S. G., Gavin, I. M. & Bradbury, E. M. Rearrangement of the histone H2A C-terminal domain in the nucleosome. *Proc Natl Acad Sci U S A* **91**, 6845-9 (1994).
68. Chadwick, B. P. & Willard, H. F. Histone H2A variants and the inactive X chromosome: identification of a second macroH2A variant. *Hum Mol Genet* **10**, 1101-13 (2001).
69. Pinto, D. M. & Flaus, A. Structure and Function of Histone H2AX. *Subcell Biochem* **50**, 55-78.
70. Redon, C. et al. Histone H2A variants H2AX and H2AZ. *Curr Opin Genet Dev* **12**, 162-9 (2002).
71. Thambirajah, A. A., Li, A., Ishibashi, T. & Ausio, J. New developments in post-translational modifications and functions of histone H2A variants. *Biochem Cell Biol* **87**, 7-17 (2009).

72. Ausio, J. Histone variants--the structure behind the function. *Brief Funct Genomic Proteomic* **5**, 228-43 (2006).
73. Nusinow, D. A. et al. Poly(ADP-ribose) polymerase 1 is inhibited by a histone H2A variant, MacroH2A, and contributes to silencing of the inactive X chromosome. *J Biol Chem* **282**, 12851-9 (2007).
74. Hansen, J. C., Tse, C. & Wolffe, A. P. Structure and function of the core histone N-termini: more than meets the eye. *Biochemistry* **37**, 17637-41 (1998).
75. Iakoucheva, L. M. et al. The importance of intrinsic disorder for protein phosphorylation. *Nucleic Acids Res* **32**, 1037-49 (2004).
76. Dyson, H. J. & Wright, P. E. Coupling of folding and binding for unstructured proteins. *Curr Opin Struct Biol* **12**, 54-60 (2002).
77. Wright, P. E. & Dyson, H. J. Intrinsically unstructured proteins: re-assessing the protein structure-function paradigm. *J Mol Biol* **293**, 321-31 (1999).
78. Rogakou, E. P., Pilch, D. R., Orr, A. H., Ivanova, V. S. & Bonner, W. M. DNA double-stranded breaks induce histone H2AX phosphorylation on serine 139. *J Biol Chem* **273**, 5858-68 (1998).
79. Redon, C. et al. Yeast histone 2A serine 129 is essential for the efficient repair of checkpoint-blind DNA damage. *EMBO Rep* **4**, 678-84 (2003).
80. Li, A. et al. Phosphorylation of histone H2A.X by DNA-dependent Protein Kinase (DNA-PK) is not affected by core histone acetylation but it alters nucleosome stability and histone H1 binding. *J Biol Chem.*
81. Dickey, J. S. et al. H2AX: functional roles and potential applications. *Chromosoma* **118**, 683-92 (2009).
82. Rogakou, E. P., Boon, C., Redon, C. & Bonner, W. M. Megabase chromatin domains involved in DNA double-strand breaks in vivo. *J Cell Biol* **146**, 905-16 (1999).
83. McManus, K. J. & Hendzel, M. J. ATM-dependent DNA damage-independent mitotic phosphorylation of H2AX in normally growing mammalian cells. *Mol Biol Cell* **16**, 5013-25 (2005).
84. Kuhne, M. et al. A double-strand break repair defect in ATM-deficient cells contributes to radiosensitivity. *Cancer Res* **64**, 500-8 (2004).
85. Formosa, T. FACT and the reorganized nucleosome. *Mol Biosyst* **4**, 1085-93 (2008).
86. Heo, K. et al. FACT-mediated exchange of histone variant H2AX regulated by phosphorylation of H2AX and ADP-ribosylation of Spt16. *Mol Cell* **30**, 86-97 (2008).
87. Keogh, M. C. et al. A phosphatase complex that dephosphorylates gammaH2AX regulates DNA damage checkpoint recovery. *Nature* **439**, 497-501 (2006).
88. Svetlova, M. P., Solovjeva, L. V. & Tomilin, N. V. Mechanism of elimination of phosphorylated histone H2AX from chromatin after repair of DNA double-strand breaks. *Mutat Res* **685**, 54-60.
89. Ausio, J., Abbott, D. W., Wang, X. & Moore, S. C. Histone variants and histone modifications: a structural perspective. *Biochem Cell Biol* **79**, 693-708 (2001).
90. Reina-San-Martin, B. et al. H2AX is required for recombination between immunoglobulin switch regions but not for intra-switch region recombination or somatic hypermutation. *J Exp Med* **197**, 1767-78 (2003).

91. Georgel, P., Demeler, B., Terpening, C., Paule, M. R. & van Holde, K. E. Binding of the RNA polymerase I transcription complex to its promoter can modify positioning of downstream nucleosomes assembled in vitro. *J Biol Chem* **268**, 1947-54 (1993).
92. Dyer, P. N. et al. Reconstitution of nucleosome core particles from recombinant histones and DNA. *Methods Enzymol* **375**, 23-44 (2004).
93. Luger, K., Rechsteiner, T. J., Flaus, A. J., Waye, M. M. & Richmond, T. J. Characterization of nucleosome core particles containing histone proteins made in bacteria. *J Mol Biol* **272**, 301-11 (1997).
94. Hansen, J. C. & Lohr, D. Assembly and structural properties of subsaturated chromatin arrays. *J Biol Chem* **268**, 5840-8 (1993).
95. Carruthers, L. M. & Hansen, J. C. The core histone N termini function independently of linker histones during chromatin condensation. *J Biol Chem* **275**, 37285-90 (2000).
96. Demeler, B. & van Holde, K. E. Sedimentation velocity analysis of highly heterogeneous systems. *Anal Biochem* **335**, 279-88 (2004).
97. Cheung, P., Allis, C. D. & Sassone-Corsi, P. Signaling to chromatin through histone modifications. *Cell* **103**, 263-71 (2000).
98. Lu, X. et al. The effect of H3K79 dimethylation and H4K20 trimethylation on nucleosome and chromatin structure. *Nat Struct Mol Biol* **15**, 1122-4 (2008).
99. Grigoryev, S. A., Arya, G., Correll, S., Woodcock, C. L. & Schlick, T. Evidence for heteromorphic chromatin fibers from analysis of nucleosome interactions. *Proc Natl Acad Sci U S A* **106**, 13317-22 (2009).